Magnetic and Mössbauer Effect Study of (Co0.5Zn0.4Cu0.1Fe2O4)(1−x)(Al2O3/PVA)x (x = 0 and 0.30) Synthesized by Sonochemical Route

ARTICLE · AUGUST 2010

CITATION
1

READS
36

3 AUTHORS, INCLUDING:

Samrat Mukherjee
Birla Institute of Technology, Mesra
13 PUBLICATIONS **95** CITATIONS
SEE PROFILE

P. K. Chakrabarti
University of Burdwan
64 PUBLICATIONS **481** CITATIONS
SEE PROFILE

Magnetic and Mössbauer Effect Study of $(Co_{0.5}Zn_{0.4}Cu_{0.1}Fe_2O_4)_{(1-x)}(Al_2O_3/PVA)_x$ ($x = 0$ and 0.30) Synthesized by Sonochemical Route

S. Mukherjee,[†] D. Das,[‡] S. Mukherjee,[§] and P. K. Chakrabarti*,[†]

Solid State Research Laboratory, Department of Physics, Burdwan University, Burdwan—713 104, West Bengal India, UGC-DAE Consortium for Scientific Research, III/LB-8, Kolkata—700 092, India, and Department of Applied Physics, Birla Institute of Technology, Mesra, Ranchi—835215, India

Received: May 18, 2010; Revised Manuscript Received: July 31, 2010

Nanoparticles of $Co_{0.5}Zn_{0.4}Cu_{0.1}Fe_2O_4$ were prepared by a combination of sonochemical and standard coprecipitation methods. The as-prepared samples were heat treated at four different temperatures to obtain particles of different sizes. The formation of the nanocrystalline phase has been confirmed by X-ray diffractograms (XRDs). The sizes of the nanoparticles have been estimated from the (311) peak of the XRD patterns using the Debye−Scherrer formula. The nanoparticles of some selected samples were coated with two different nonmagnetic matrices, viz., alumina (Al_2O_3) and poly(vinyl alcohol) (PVA). Results of high-resolution transmission electron microscopy observations of some samples are in agreement with those extracted from the XRD data. The inclusion of sonochemical technique in the coprecipitation method reduces the distribution of sizes of nanoparticles. The static magnetic properties have been measured with maximum applied field of 2 T, and the dynamic magnetic properties have also been observed at room temperature using different time windows. The static and dynamic magnetic properties of all the samples confirmed the presence of ferrimagnetic and superparamagnetic (SPM) particles. The saturation magnetizations at room temperature of the samples are high, and coercive fields are also low. Mössbauer spectra of the samples recorded at room temperature are composed of relaxing sextet along with the signature of doublet which suggests the presence of ferrimagnetic particles along with SPM particles. The SPM relaxations of the samples annealed at higher temperature have been enhanced by encapsulating the nanoparticles in nonmagnetic matrix of Al_2O_3 and PVA with 30% coating.

Introduction

Investigations of the nanosized mixed spinel ferrites are the subject of intense research due to their large departure of physical properties from those of their bulk counterparts.[1−9] Besides, magnetic nanoparticles of ferrites are technologically important materials for their use in high-density magnetic information storage,[10,11] magnetic fluid, magnetoresponsive colloidal extractants,[12] targeted drug delivery vectors for gene therapy, genetic screening, biochemical, toxicity cleansing,[13−16] in vivo imaging and contrast agents,[17] magnetocytolysis agents for treatment of localized cancerous tumors,[17−24] magnetic cell sorting schemes,[22] etc. The spinel ferrites are also suitable for various applications in the microwave domain with frequency ranging from 3 to 30 GHz.[25,26] In this direction some mixed spinel ferrites have been used in multilayer chip inductors (MLCIs), which have drawn much attention for their applications in communicative electronic devices .[27,28] Among the spinel ferrites, soft magnetic ferrites with very low coercive field, low loss, as well as large resistivity and large magnetic moment in the superparamagnetic (SPM) state, are interesting for their multidimensional applications in various electromagnetic devices.[6,9,29] The saturation magnetization and the coercivity are strongly dependent on the annealing temperatures and are directly related to the variation of particle sizes.[25,30] In the ferrite family, the well-studied member is the cobalt ferrite $CoFe_2O_4$. Various works on cobalt ferrite have been reported; viz., Mata-Zamora et al.[25] investigated the nonresonant microwave application of cobalt ferrite nanoparticles. Victoria et al.[31] reported on the synthesis and magnetic characterization of cobalt-substituted ferrite ($Co_xFe_{3-x}O_4$) nanoparticles. García-Cerda et al.[32] reported on the preparation and characterization of poly(vinyl alcohol)−cobalt ferrite nanocomposites. Various conventional methods such as coprecipitation, thermal decomposition, sol−gel, and hydrothermal methods have been widely used. To improve the magnetic properties of the Co-ferrite, in the present paper we have considered the substitution of Zn and Cu ($Co_{0.5}Zn_{0.4}Cu_{0.1}Fe_2O_4$, CZCF), and to the authors' knowledge, no work on this composition of CZCF ferrite has been reported earlier. The sonochemical technique has been included in the conventional coprecipitaion method, and the as-prepared sample is heat-treated at different temperatures. Some selected samples were incorporated in two nonmagnetic matrices, viz., alumina (Al_2O_3) and poly(vinyl alcohol) (PVA), which are CZCFA [$(Co_{0.5}Zn_{0.4}Cu_{0.1}Fe_2O_4)_{(1-x)}(Al_2O_3)_x$ ($x = 0.30$)] and CZCFP [$(Co_{0.5}Zn_{0.4}Cu_{0.1}Fe_2O_4)_{(1-x)}(PVA)_x$ ($x = 0.30$)]. X-ray diffractograms (XRD) and high-resolution transmission electron microscopy (HRTEM) were observed to characterize the different samples. Static magnetic measurements were carried out with maximum applied field of 2 T. The ac magnetic and Mössbauer effect measurements of all the samples were also carried out. Magnetic (dc and ac) and Mössbauer studies indicate the presence of ferrimagnetic nanoparticles along with SPM

* To whom correspondence should be addressed. E-mail address: pabitra_c@hotmail.com. Tel.: 0091 342 2657800. Fax: 0091 342 2530452.
[†] Burdwan University.
[‡] UGC-DAE Consortium for Scientific Research.
[§] Birla Institute of Technology.

10.1021/jp104535v
Published on Web 08/19/2010

relaxations of the magnetic nanoparticles. Also, some interesting results were found from the magnetic and Mössbauer studies.

Experimental Methods

Mixed spinel $Co_{0.5}Zn_{0.4}Cu_{0.1}Fe_2O_4$ was prepared by combination of sonochemical and standard coprecipitation methods. Anhydrous ferric chloride ($FeCl_3$), cobalt chloride ($CoCl_2$), anhydrous zinc chloride ($ZnCl_2$), and copper chloride ($CuCl_2$) were used as starting materials. A complete homogeneous solution of all the four starting materials was prepared by triple-distilled water. A few drops of hydrochloric acid were added to obtain a clear solution. The stoichiometric ratio of Co, Zn, Cu, Fe is taken as 0.5:0.4:0.1:2. The prepared solution is then sonicated for half an hour. For coprecipitation, dilute NaOH solution was added dropwise to the salt solution at 80 °C, and the final pH was kept at 10. During the slow addition of NaOH, ultrasonication was continued and maintained for about 2 h during the whole course of coprecipitation. To obtain a neutral pH condition as well as to remove the extra ions, the precipitated particles were filtered and washed several times by triple-distilled water. Finally, the precipitated particles were dried at 100 °C for 12 h. The as-prepared samples were then annealed at 400, 600, 800, and 1000 °C to obtain different particle sizes. In the next step certain amounts of as-prepared CZCF sample were coated with Al_2O_3, i.e., CZCFA. For the preparation of CZCFA, aluminum nitrate nonahydrate salt was used as a precursor material for alumina and NaOH was used for its precipitation in aqueous solution. The salt was dissolved in triple-distilled water, and CZCF particles were added to it. To make the homogeneous dispersion of CZCF particles in salt solution, sonication was given for half an hour. NaOH solution was added slowly for the precipitation of the salt, and the final pH of the solution was kept at 9. For complete precipitation and digestion, sonication was further continued for an hour after completion of NaOH addition. The precipitate was washed several times by decantation for neutralization and for the removal of the extra ions. The finally obtained nanocomposite was dried and annealed at 600 °C (CZCFA). For the preparation of the nanocomposite of CZCFP, the PVA was taken in triple-distilled water and the solution was prepared under boiling condition. The nanoparticles of the as-prepared CZCF were uniformly dispersed in water in another beaker under sonication. These uniformly dispersed CZCF particles were then slowly added to the PVA solution under boiling condition, and the boiling condition was maintained thoroughly until the whole nanocomposite was dried. Finally, the sample of CZCFP was collected in powder form. XRD patterns of all the samples were taken in an Xpert Pro Phillips XRD unit with Co radiation (λ = 0.178 897 nm) in the range of 2θ from 10 to 100°. The quantitative amount of Co, Zn, Cu, and Fe ions of some samples has been measured by ICP OCS, and the stoichiometric ratio has been estimated from the observed data. HRTEM pictures were taken in a JEOL JEM 2100 HRTEM, Japan, resolution = 1.9 Å. Digital hysteresis loops at different frequencies were observed by using a digital hysteresis loop tracer supplied by Metis Instruments and Equipments NV, Belgium. Mössbauer effect measurements were carried out by using a PC-based spectrometer having a 1024 channels MCA card operating in the constant acceleration mode. All measurements were carried out in transmission geometry using a 10 mCi ^{57}Co source in Rh matrix. The details of our Mössbauer effect measurements were given in our earlier papers.[7,8,33] Static magnetic measurements were carried out in a Quantum design SQUID Magnetometer.

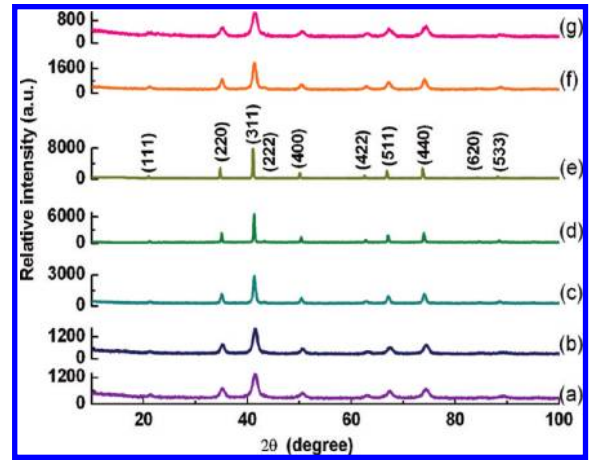

Figure 1. XRD patterns of CZCF samples: (a) as-prepared; (b) T_A = 400 °C; (c) T_A = 600 °C; (d) T_A = 800 °C; (e) T_A = 1000 °C; (f) CZCFA, T_A = 600 °C (30% Al_2O_3 coating); (g) CZCFP, as prepared (30% PVA coating).

Results, Analysis, and Discussion

XRD and TEM Analyses. X-ray diffraction patterns of all the annealed samples (Figure 1) confirmed the formation of the mixed spinel $Co_{0.5}Zn_{0.4}Cu_{0.1}Fe_2O_4$ phase of the samples. No other peak except the desired phase is observed in the samples annealed at different temperatures. All the peaks are assigned using JCPDS file (No. 22-1086). It is interesting to note that spinel ferrite phase has been formed even in the as-prepared sample dried at 100 °C. The average particle sizes of all the samples were calculated from the line broadening of the (311) peak of the XRD pattern using the well-known Debye−Scherrer equation $\langle D \rangle_{(311)} = (0.9\lambda)/(\beta_{1/2} \cos \theta)$, where the symbols have their usual meanings.[33] The average particle size of all the samples lies in the range 5.6−50.3 nm. The lattice parameters of all the samples were calculated by considering all the peaks in the XRD pattern after performing Nelson−Riley−Taylor−Sinclair correction in order to compensate the peak shift due to sample offset. Lattice parameters and particle sizes are shown in Table 1. The variation of the lattice parameter as a function of annealing temperature including the error bars is shown in Figure 2. From this figure it is clear that the lattice parameter of the CZCF sample annealed at 400 °C is slightly higher than that of the as-prepared sample (Table 1). But above 400 °C and up to 800 °C, the lattice parameter increases steadily, and beyond 800 °C, it increases very slowly. This type of variation may be attributed to the redistribution of cations between the tetrahedral and octahedral sites of the cubic lattice of the spinel ferrite.[33] We have tested three samples (as-prepared and annealed (400 and 600 °C) samples of CZCF) by ICP OCS for the estimation of the stoichiometric ratio of Co, Zn, Cu, and Fe ions. The number of Co, Zn, Cu, and Fe ions has been calculated from their respective amounts extracted from the observed data, and the average number of Cu, Co, Zn, and Fe ions for three samples are, respectively, 1000x, 5410x, 3510x, and 22 630x; here x is a common multiplication factor and the corresponding stoichiometric ratio of Co, Zn, Cu, and Fe ions is 0.541:0.351:1.000:2.263. There is a slight variation from our chosen stoichiometric ratio, but the obtained results are more-or-less satisfactory. The degree of cationic inversion normally depends on the size of the nanoparticle, method of preparation, annealing temperature, etc.[34] The particle size increases with the increase of annealing temperature (T_A), which is expected due to the increase of crystalline state at higher temperature. However, this is not applicable in the case of CZCFA, which is annealed at

TABLE 1: Heat Treatment Schedule, Lattice Parameters, and Average Particle Sizes of CZCF, CZCFA, and CZCFP Samples

samples	composition	annealing temperature (°C)	lattice parameter (nm)	average particle sizes (nm) XRD	TEM
CZCF		as-prepared	8.3844	5.6	6.7
		400	8.3782	10.3	
	$Co_{0.5}Zn_{0.4}Cu_{0.1}Fe_2O_4$	600	8.4070	19.5	
		800	8.4091	46.8	
		1000	8.4571	50.3	
CZCFA	$(Co_{0.5}Zn_{0.4}Cu_{0.1}Fe_2O_4)_{0.70}(Al_2O_3)_{0.30}$	600	8.4015	12.4	13.5
CZCFP	$(Co_{0.5}Zn_{0.4}Cu_{0.1}Fe_2O_4)_{0.70}(PVA)_{0.30}$	not yet annealed	8.3641	9.1	9.4

higher temperature (T_A = 600 °C). From the sizes of nanoparticles of CZCF and CZCFA, it is evident that the growth of nanoparticles is being restricted when the particles are encapsulated by nonmagnetic matrix of alumina. HRTEM images of the CZCF, CZCFA annealed at 600 °C, and CZCFP are shown in Figure 3. The particle size of CZCFP is more compared to the as-prepared CZCF, although the annealing temperature is the same. This may be due to the effect of encapsulation of the CZCF particles by PVA matrix. In many cases of nanocrystalline ferrites, it is found that there is a tendency of agglomeration among the nanoparticles; in the present system the micrographs of the particles displayed in Figure 3a, c, and e are well-dispersed nanoparticles, i.e., the particles are not yet agglomerated in the present case. It is evident from the overall view of the micrographs of the as-prepared CZCF (Figure 3a), CZCFA annealed at 600 °C (Figure 3c), and CZCFP (Figure 3e) that the nanoparticles are more or less of uniform sizes. But the distribution of particle size of CZCFP is comparatively wide compared to the other two cases, and this is due to the fact that in this case we could not maintain the sonication during the encapsulation by PVA under boiling condition. To estimate the average particle size of all the samples, we have measured the diameter in different direction of a given nanoparticle. To get the size distribution of the nanoparticles and hence to draw the histogram, we have measured the average size of a large number of nanoparticles selected from the different observed micrographs of all the samples. The distributions of particle sizes of CZCF, CZCFA, and CZCFP samples obtained from the results of the measured average diameters of the nanoparticles are displayed in the histograms (Figure 3b, d, f). The average diameter of the maximum number of particles present in the as-prepared sample of CZCF lies between 5 and 8 nm. But for the nanocomposite sample of CZCFA annealed at the same temperature, i.e., 600 °C, the average diameter of the maximum number of particles lies in the range of 9−10 nm. The average particle size of the as-prepared sample of CZCF obtained from the micrographs is ∼6.7 nm and for the CZCFP sample (which is also prepared using the as-prepared CZCF sample), the average size is ∼9.4 nm, which is greater than that of the CZCF sample. The above difference may be due to the increase of sizes of CZCF particles during the course of the coating with PVA under boiling condition. The average particle size of the coated particles of CZCFA sample annealed at 600 °C obtained from the micrographs is ∼13.5 nm, which is much less than the CZCF (19.5 nm) sample annealed at the same T_A (particle size calculated from XRD). In all the cases of CZCF and CZCFA annealed at 600 °C and CZCFP sample, the average sizes obtained from TEM micrographs are in good agreement with those calculated from the XRD pattern (Table 1). Thus small particles of $Co_{0.5}Zn_{0.4}Cu_{0.1}Fe_2O_4$ can be formed even at higher annealing temperature, when the particles are encapsulated by the nonmagnetic alumina matrix. Structural information of all the samples investigated in HRTEM has also been revealed from the single crystalline lattice fringes and selected area electron diffraction (SAED) patterns. In the fringe pattern displayed in Figure 3g of the nanoparticle, it is evident that the lattice fringes correspond to a group of atomic planes within the nanoparticle, indicating that the particle is of single crystalline with no defect. The distance between the two adjacent planes is calculated and its value is ∼0.483 nm, which corresponds to the (111) plane of the $Co_{0.5}Zn_{0.4}Cu_{0.1}Fe_2O_4$ nanocrystallite. From the coated nanoparticles displayed in Figure 3c, it is evident that the particle is well-coated. But in the case of CZCFP, the particles are found to disperse in the PVA matrix. A representative SAED pattern acquired from a nanoparticle of CZCFA sample annealed at 600 °C is shown in Figure 3h. The different lattice planes in the SAED pattern are assigned, and these are in good agreement with the present mixed spinel system.

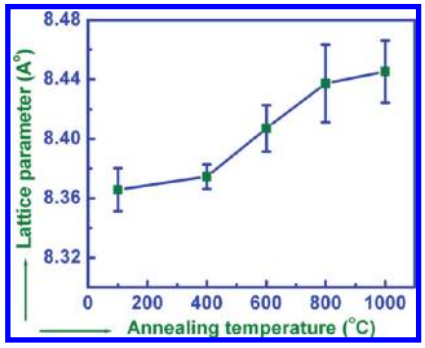

Figure 2. Variation of lattice parameters with annealing temperature of CZCF samples.

Magnetic Properties. ***ac Magnetic Properties.*** The dynamic magnetization of all the samples was measured at different frequencies, and the maximum ac magnetic field applied in the measurement of ac magnetization was ∼60 kA/m. But the maximum ac magnetic field was lower in the case of high-frequency measurements. The dynamic magnetization of all the samples increases nonlinearly with the increase of ac excitation (Figure 4). This suggests that the magnetic behavior of these samples is controlled by the ferrimagnetic particles. Also, the nonlinear magnetization curves suggest that most of the particles in these samples are interacting. But the rate of increase of magnetization with the increase of ac excitation of all these samples is relatively slow compared to usual behavior of soft magnetic particles. This type of behavior is due to the presence of SPM particles together with the ferrimagnetic particles.

Dynamic hysteresis loops of all the samples in the frequency range of 5−400 Hz have been observed, and different magnetic properties, viz., coercive field, maximum magnetization to remanence ratio, magnetic losses, etc., were extracted from the observed hysteresis loops. The ac loops observed at 50 Hz of all the samples are displayed in Figure 5. The coercivity of the samples increases with the increase of particle size. This is due

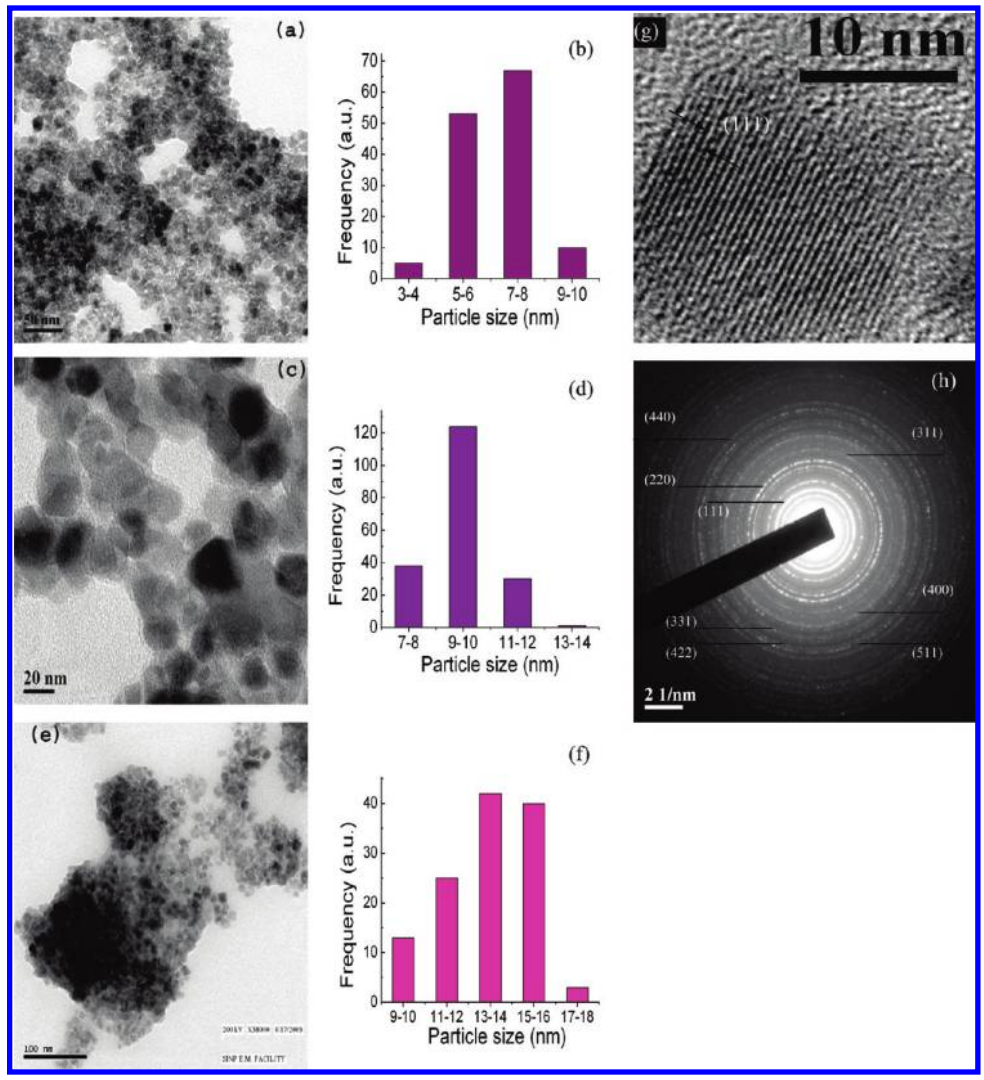

Figure 3. HRTEM results of the CZCF, CZCFA, and CZCFP samples: (a) micrograph (CZCF, as-prepared); (b) histogram (CZCF, as-prepared); (c) micrograph (CZCFA, $T_A = 600$ °C); (d) histogram (CZCFA, $T_A = 600$ °C); (e) micrograph (CZCFP, not yet annealed); (f) histogram (CZCFP, not yet annealed); (e) fringe patterns (CZCFA, $T_A = 600$ °C); (g) SAED pattern (CZCFA, $T_A = 600$ °C).

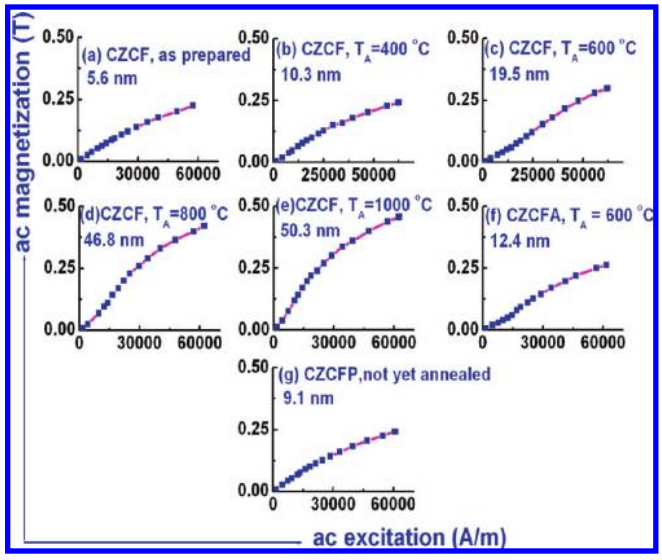

Figure 4. Variation of magnetization with excitation of the CZCF samples: (a) as-prepared; (b) $T_A = 400$ °C; (c) $T_A = 600$ °C; (d) $T_A = 800$ °C; (e) $T_A = 1000$ °C; (f) CZCFA, $T_A = 600$ °C (30% Al_2O_3 coating); (g) CZCFP, not yet annealed (30% PVA coating).

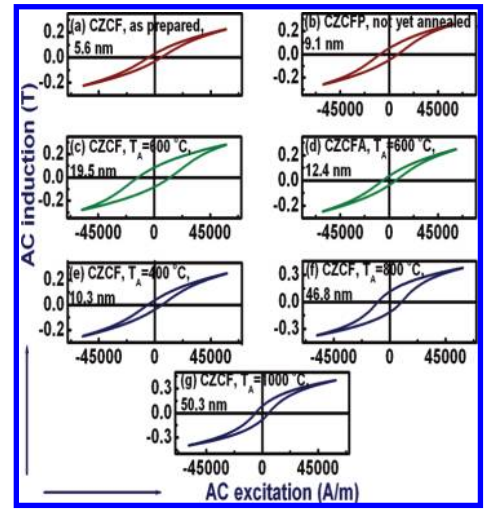

Figure 5. Hysteresis loops observed at 50 Hz of the CZCF samples: (a) as prepared; (b) CZCFP, not yet annealed (30% PVA coating); (c) $T_A = 600$ °C; (d) CZCFA, $T_A = 600$ °C (30% Al_2O_3 coating); (e) $T_A = 400$ °C; (f) $T_A = 800$ °C; (g) $T_A = 1000$ °C.

to the increase of the fraction of ferrimagnetic particles compared to those of SPM particles. This feature is also well supported from the Mössbauer spectra of these samples discussed in the next section. All the observed loops are minor loops as the maximum ac field is not enough to reach the

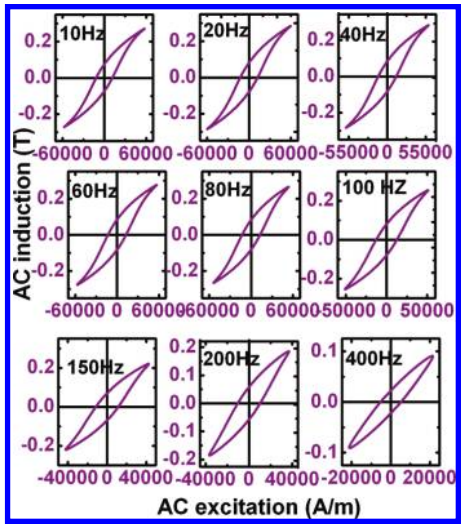

Figure 6. Hysteresis loops of CZCF annealed at 600 °C for different frequencies.

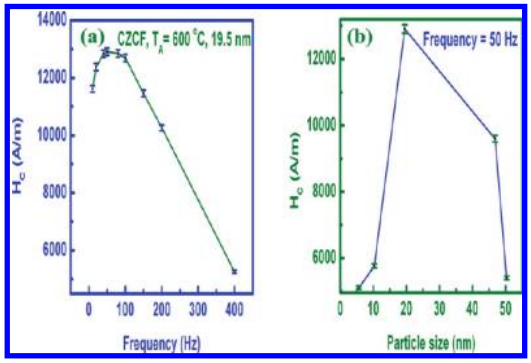

Figure 7. Variation of coercive field with (a) frequency of CZCF, annealed at 600 °C; (b) particle size ($f = 50$ Hz).

saturation. The hysteresis loops of the samples are getting their typical shapes with the increase of particle size. The hysteresis loops of all the samples were recorded at different frequencies, and one representative loop of the sample of CZCF annealed at 600 °C is shown in Figure 6. The value of maximum induction (B_m) of the uncoated sample is a bit high compared to that of the coated sample though the annealing temperature is the same. This is due to the presence of nonmagnetic fraction in the coated sample. There is a decrease in coercive field with the decrease of frequency of observations, i.e., with the increase of experimental time window. This is due to the SPM relaxations of the nanoparticles of all the samples. The variation of loss with the frequency (not shown here) showed that the hysteresis loss of a given particle size sample increases with the increase of frequency. On the other hand, for a given frequency the hysteresis loss increases with the increase of particle size. The variation of coercive field with the frequency for a given particle size (19.5 nm) sample and the variation of coercive field with particle size for a given frequency (50 Hz) are shown in Figure 7. In all cases, the coercive field increases with the increase of particle size. This fact is due to the lowering of the measuring time window with the increase of frequency. In the case of nanoparticle system with uniaxial anisotropy, the energy barrier, which separates the two easy directions of magnetization, may be smaller than the thermal energy even at room temperature, which leads to spontaneous fluctuation of the magnetization direction having relaxation time given by[33]

$$\tau = \tau_0 \exp\left(\frac{KV}{k_B T}\right)$$

Here τ_0 ($10^{-9}-10^{-10}$ s) is the inverse of the natural frequency of the gyromagnetic precession, K is the anisotropy energy constant, V is the volume of the particle, k_B is the Boltzmann constant, and T is temperature in K. As we increase the frequency, the value of τ, the measuring time window, decreases; consequently, the difference of relaxation time and measuring time window decreases. The particles which behave superparamagnetic at a given frequency, say, 50 Hz, may behave as ferrimagnetic ordered particles at higher frequency, say, 100 Hz. Thus once we increase the frequency, the number of SPM particles decreases and at the same time the number of ferrimagnetic particles increases. Due to this fact, ac hysteresis loops become wider and wider with the increase of frequency. We have also extracted the values of the ratio of maximum magnetization and remanance (B_m/B_r) from the dynamic loops of all the samples. For a given sample, the ratio decreases with the increase of frequency.

dc Magnetic Properties. Static (dc) hysteresis loops of CZCF samples annealed at 400, 600, and 800 °C and CZCFA observed at 300 K are displayed in Figure 8. The hysteresis loops for the samples of CZCF annealed at 400 and 600 °C and CZCFA observed at 300 K are not saturated even when a field of 2 T is applied. This is due to the fact that these samples consist of both ferrimagnetic and SPM particles. But the hysteresis loop of CZCF annealed at 800 °C is more or less saturated within the limit of the applied maximum field (2 T). This suggests that most of the particles of this sample are ferrimagnetic. We have extracted the positive and negative values of coercive field (H_c) from each loop recorded at 300 K, and the values of H_c have been estimated from their average. It is true that there is a small difference between the positive and negative values of H_c which may be due to the exchange bias effect. The variations of coercive field extracted from the loops recorded at 300 K, with the particle size of CZCF samples annealed at 400, 600, and 800 °C and CZCFA sample, are shown in Figure 9a. The lowest coercive field of 5.9 G has been found in the case of CZCF sample annealed at 400 °C (at 300 K). The coercive fields (H_c) extracted from these loops recorded at 300 K of CZCF samples annealed at 600, 800 °C and CZCFA sample are, respectively, 81.6, 72.3, and 8.2 G. From the results of uncoated and coated samples annealed at 600 °C, it is clear that the value of H_c is drastically reduced in the case of coated sample although the annealing temperature in both the cases is the same. This is due to the encapsulation of the magnetic nanoparticle by the matrix of alumina which restricts the particle growth at higher annealing temperatures. This would be suitable for soft magnetic applications. Also, the values of H_c of these samples are very low compared to that of the corresponding bulk state. The low value is due to the presence of SPM particles. The value of the maximum magnetization of CZCF annealed at 600 °C measured at 300 K is 67 emu/g (for the applied field at 2 T), which is greater than that of the coated sample of CZCFA annealed at 600 °C (~62 emu/g). The maximum magnetization at 300 K obtained in the case of CZCF sample annealed at 800 °C is 82.4 emu/g. The value of saturation magnetization of $Co_{0.5}Zn_{0.5}Fe_2O_4$ sample with particle size 30−50 (annealed at 1000 °C) is 71 emu/g.[35] This sample is annealed at higher temperature, and the particle size is also high compared to our sample of CZCF annealed at 800 °C. But the magnetization of our sample is quite high and at the same time the coercive field is surprisingly low because of the presence of a small fraction

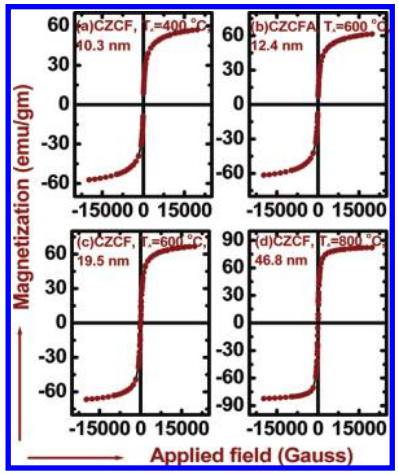

Figure 8. dc hysteresis loops recorded at 300 K of (a) CZCF annealed at 400 °C; (b) CZCFA annealed at 600 °C; (c) CZCF annealed at 600 °C; (d) CZCF annealed at 800 °C.

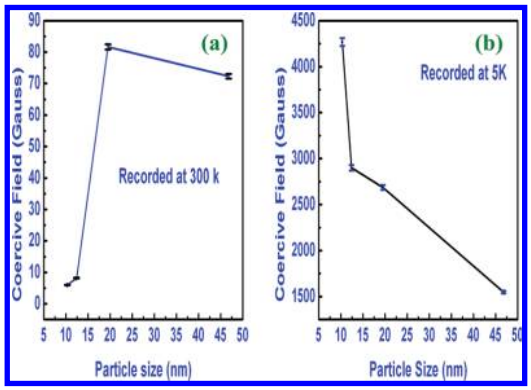

Figure 9. Variation of coercive field with particle size (a) at 300 K; (b) at 5 K.

of SPM particles together with the ferrimagnetic particles as the annealing temperature is low. Hence it can be stated that the present composition gives a moderately high value of saturation magnetization. Actually the substitution of Zn and Cu in Co-ferrite reduce the nanocrystalline anisotropy as well as the coercive field. Due to the lowering of magnetocrystalline anisotropy, the onset of SPM relaxation at room temperature would favor even when the particle size is more. That is, bigger size particles can exhibit SPM relaxations at higher temperature, and consequently the blocking temperature would be high. Also, the mixed state of the present system reduces the coercive field, and this sample is also interesting for the square shape of the present loop. In our previous investigation we have prepared and investigated magnetic properties of many mixed spinel SPM nanocrystalline ferrites including nanocomposites which are Zn-substituted Mg-ferrite [$Mg_{(1-x)}Zn_xFe_2O_4$ ($x = 0.15$, 0.30, and 0.50)],[7] $Ni_{0.2}Zn_{0.6}Cu_{0.2}Fe_2O_4$,[33] $Ni_{0.4}Zn_{0.4}Cu_{0.2}Fe_2O_4$,[36] $(Ni_{0.2}Zn_{0.6}Cu_{0.2}Fe_2O_4)_{(1-x)}(Al_2O_3)_x$ ($x = 0.15$, 0.30, 0.45),[37] $(NiFe_2O_4)_{1-x}(Al_2O_3)_x$ ($x = 0.25$, 0.40),[38] $(Mn_{0.4}Zn_{0.6}Fe_2O_4)_{1-x}(SiO_2)_x$ ($x = 0.9$, 0.15, 0.25),[39] etc. Also several investigations on these types of systems have been reported by various workers in recent times.[40−46] Considering all these systems, it can be stated that the investigations reported on the present composition are particularly interesting as far as maximum/saturation room temperature magnetization including low coercive field as well as low hysteresis loss and shapes are concerned. Thus the present samples with moderately high value of magnetization, low coercive field, and hysteresis loss including the shape of the hystereis loop would be appropriate for applications in various electromagnetic devices.

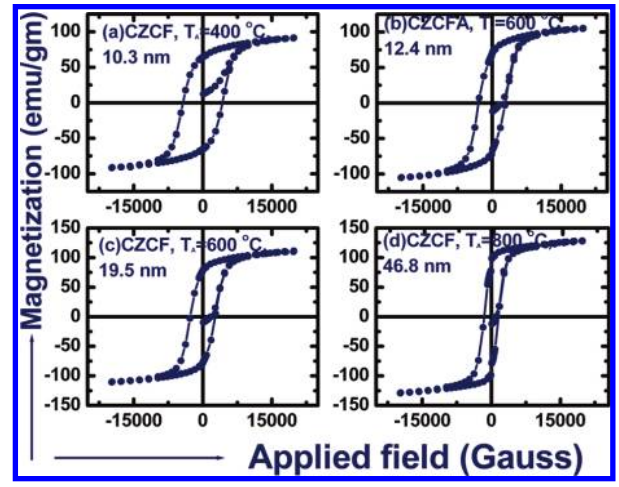

Figure 10. dc hysteresis loops recorded at 5 K of (a) CZCF annealed at 400 °C; (b) CZCFA annealed at 600 °C; (c) CZCF annealed at 600 °C; (d) CZCF annealed at 800 °C.

The static hysteresis loops of all the samples investigated by a SQUID magnetometer observed at 5 K (Figure 10) are significantly different from those recorded at 300 K (Figure 8). All these observed loops at 5 K are wide, which indicates that coercive fields of all the samples have substantially enhanced due to the fact that most of the particles which are SPM at room temperature become ferrimagnetic at 5 K. The variation of coercive field extracted from the loops recorded at 5 K, with the particle size of CZCF samples annealed at 400, 600, and 800 °C and CZCFA sample, are shown in Figure 9b. The lowest coercive field of 1548 G has been found in the case of CZCF sample annealed at 800 °C. The coercive field (H_c) extracted from these loops recorded at 5 K of CZCF samples annealed at 400, 600 and CZCFA sample are, respectively, 4267.3, 2688.3, and 2899.9 G. Thus the lowest value of coercive field of the sample CZCF annealed at 800 °C (1548.6 G) has been increased by a multiplication factor of 21.5 as the temperature is lowered from 300 to 5 K. But the multiplication factor of all the samples is not equal. This difference may be due to various reasons, viz., unequal change of nanocrystalline anisotropy with lowering of temperature, particle shape, size, and their distribution. The maximum magnetization extracted from the dc loops recorded at 5 K of all the samples increases substantially from those extracted from the loops recorded at 300 K. The value of the maximum magnetization of CZCF annealed at 600 °C measured at 5 K is 111.3 emu/g (for the applied field at 2 T), which is greater than that of the coated sample of CZCFA annealed at 600 °C (105.3 emu/g). Thus for a given sample, maximum magnetization increases with the lowering of temperature. This increase of magnetization is due to increase of the fraction of ordered ferrimagnetic particles at the cost of SPM particles. Another factor for the increase of magnetization may be due to the lowering of the magnetocrystalline anisotropy with the lowering of temperature. In the nanoparticle state of all the present samples, the room temperature magnetization has been found to be enhanced compared to the previously reported values.[35,47] Thus, with the lowering of temperature the magnetic properties of the nanoparticle system are not dictated only by the composition. Rather various other characteristic features of the nanoparticle systems, viz., nanoparticle size, shape, distribution, shape anisotropy, etc., are also responsible for the change of the magnetic behavior. SQUID measurements of these samples have also confirmed that SPM behavior of the nanocomposite system (CZCFA) has been enhanced by encapsulating the particles in a nonmagnetic host, and this is in agreement

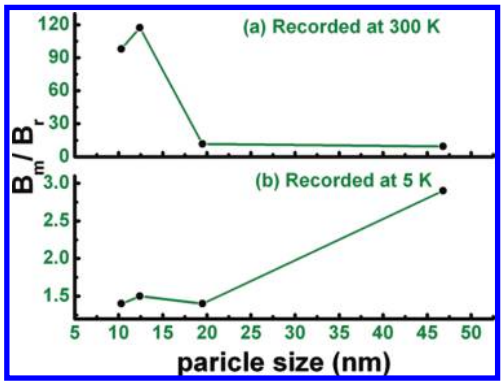

Figure 11. Variation of $(B_m/B_r)_{dc}$ with particle size (a) at 300 K; (b) at 5 K.

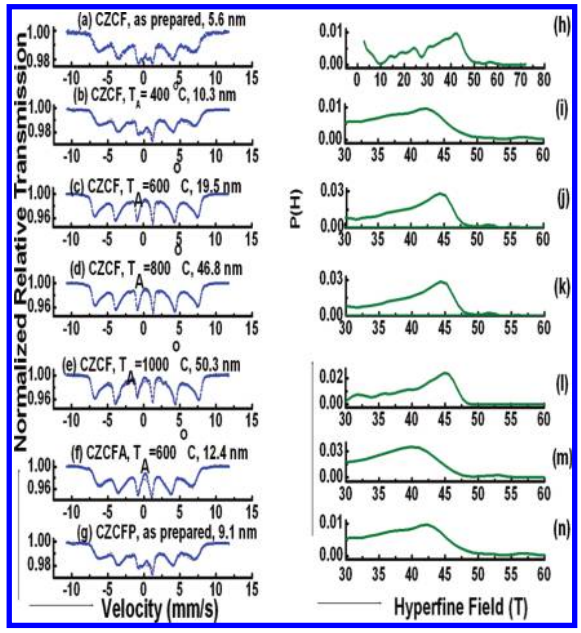

Figure 12. Mössbauer spectroscopy of CZCF samples: (a) as-prepared; (b) $T_A = 400$ °C; (c) $T_A = 600$ °C; (d) $T_A = 800$ °C; (e) $T_A = 1000$ °C; (f) CZCFA, $T_A = 600$ °C (30% Al_2O_3 coating); (g) CZCFP, not yet annealed (30% PVA coating). Distribution of hyperfine fields of the CZCF samples: (h) as-prepared; (i) $T_A = 400$ °C; (j) $T_A = 600$ °C; (k) $T_A = 800$ °C; (l) $T_A = 1000$ °C; (m) CZCFA, $T_A = 600$ °C (30% Al_2O_3 coating); (n) CZCFP, not yet annealed (30% PVA coating).

with our dynamic magnetic studies. All the loops recorded at 5 K of all the samples are not strictly saturated with maximum field of ~2 T, and this sort of behavior may be due to the presence of very small particles whose blocking temperatures (T_B) are still lower than the lowest temperature attained in this study. The variations of $(B_m/B_r)_{dc}$ measured at 5 and 300 K as a function of particle size of the sample are shown in Figure 11. On the other hand, the ratio of $(B_m/B_r)_{dc}$ measured at 5 K for a given sample increases from its room temperature value. This result suggests that the shape of the loop becomes square as we lower the temperature of measurement.

Mössbauer Analysis. The Mössbauer spectra of all the samples (as-prepared CZCF, CZCF annealed at 400, 600, 800, and 1000 °C, CZCFA annealed at 600 °C, and CZCFP) are shown in Figure 12. Figure 12a represents the Mössbauer spectrum of the as-prepared CZCF, and this pattern is different from those of the others (Figure 12b−e). Although the average size of the as-prepared sample is very low (only 5.6 nm), the Mössbauer pattern is not a pure doublet. Rather this pattern contains a relaxing sextet together with a prominent doublet in the central region. The doublet is assigned to SPM particles, and the sextet is assigned to the ordered ferrimagnetic particles. A close inspection of the spectrum shows that the area of the sextet pattern is comparatively less than that of the doublet. With the increase of particle size, the intensity of the sextet pattern increases while the intensity of the doublet pattern decreases. Parts b−e of Figure 12 represent the Mössbauer spectra of CZCF samples annealed at 400, 600, 800, and 1000 °C (average particle sizes are, respectively, 10.3, 19.5, 46.8, and 50.3 nm). These spectra are composed of relaxing sextet corresponding to the ferrimagnetic ordered particles together with a weak signature of doublet corresponding to the SPM particles. For these samples Mossbauer spectra suggest that we are far below the blocking temperature as far as Mössbauer time window is concerned. The Mössbauer spectra displayed in Figure 12f, g of CZCFA and CZCFP samples also show a mixture of doublet together with a relaxing sextet. Parts c and f of Figure 12 represent the Mössbauer spectra of uncoated (CZCF) and coated (CZCFA) samples which were annealed at the same temperature (600 °C). However, the annealing temperature is the same, but the Mössbauer spectra of these samples are interestingly different from each other. In the coated sample the doublet intensity is more compared to that of the uncoated one. This is mainly due to the abnormal reduction of growth of the nanoparticles by the coating materials. Thus the coating materials not only modulate the exchange interaction among the ferrimagnetic particles but they substantially reduce the particle growth of the sample. The low values of particle sizes of some samples (as-prepared and annealed (400 °C) samples of CZCF and CZCFP) estimated from the XRD and TEM pictures suggest the presence of quadrupolar doublet in the Mössbauer spectra. But instead of doublet, the Mössbauer spectra of these samples are composed of magnetic sextet together with quadrupolar doublet pattern. From this fact, it is to be noted that the sizes of some fraction of particles of these samples are more than the critical size corresponding to the Mössbauer time window. These particles give the magnetic sextet pattern along with the doublet pattern of the SPM particles.

All the Mössbauer spectra of the samples were fitted using the NORMOS program for distribution of hyperfine fields along with a quadrupole doublet.[48] The doublets in these patterns are

TABLE 2: Hyperfine Parameters Extracted from the Mössbauer Spectra Recorded at Room Temperature of CZCF, CZCFA, and CZCFP Samples

sample	composition	annealing temperature (°C)	IS (mm/s)	QS (mm/s)	mean hyperfine field (T)
CZCF	$Co_{0.5}Zn_{0.4}Cu_{0.1}Fe_2O_4$	as-prepared	0.39	0.33	35.09
		400	0.39	0.36	33.76
		600	0.33	0.07	37.57
		800	0.38	0.16	39.37
		1000	0.38	0.26	40.92
CZCFA	$(Co_{0.5}Zn_{0.4}Cu_{0.1}Fe_2O_4)_{0.70}(Al_2O_3)_{0.30}$	600	0.23	0.13	35.07
CZCFP	$(Co_{0.5}Zn_{0.4}Cu_{0.1}Fe_2O_4)_{0.70}(PVA)_{0.30}$	not yet annealed	0.42	0.01	30.23

due the ultrafine ferrite nanoparticles undergoing SPM relaxation, whereas the relaxing sextets are due to the particles having relaxation time close to the characteristic time scale of Mössbauer measurement ($\sim 10^{-8}$ s) having a size distribution. The probability distributions of the hyperfine magnetic field $P(H)$ as a function of the internal hyperfine magnetic field H are shown in Figure 12h−n. In the case of uncoated CZCF samples, broad peaks have been observed with maximum hyperfine field at 42.3, 42.5, 44.3, 44.5, and 45.3 T for the particles with size 5.6, 10.3, 19.5, 46.8, and 50.3 nm, respectively. These well-defined peaks indicate a bit less size distribution of the nanoparticles of the present samples compared to the samples studied earlier by our group.[33] In the case of coated samples (CZCFA and CZCFP), the distribution of hyperfine field also shows broad peaks but with less number of maxima; the maxima are at 39.7 and 42.2 T, respectively. The hyperfine parameters extracted from the fit are tabulated in Table 2. The values of isomer shift (IS) extracted from the fit (Table 2) confirmed the Fe^{3+} valence state of iron in the ferrites, whereas the QS values, extracted from the fitting of the relaxing sextet, are indicative of substantial electric field gradient (EFG) around the ^{57}Fe probe nuclei.[33]

Conclusion

The single phase nanoparticles/nanocomposite mixed spinel ferrites (CZCF, CZCFA, and CZCFP) have been prepared by the combination of chemical coprecipitation and ultrasonication. Interestingly, no unwanted phase has been formed even at high annealing temperature, i.e., 1000 °C. The introduction of ultrasonic vibration during the course of coprecipitation for the preparation of nanoparticle systems (CZCF and CZCFA) drastically reduces the distribution of sizes. Encapsulation of the magnetic nanoparticles by nonmagnetic matrix (Al_2O_3) restricts the growth of nanoparticles at higher annealing temperature. This fact also suggests the well encapsulation of the nanoparticles in the present method of preparation of coated nanoparticles where the precursor salt of the coating material (here aluminum chloride) has been precipitated in the presence of ferrite particles. Results of HRTEM observations of the samples are in good agreement with those extracted from the XRD. The results of dynamic and static magnetic measurements indicate that the present samples are in the mixed state of SPM and ferrimagnetic particles. The fraction of ferrimagnetic particles of the samples annealed at different temperatures increases with the increased annealing temperature. These findings are in good agreement with those obtained from the Mössbauer spectra. The restricted growth of particles, i.e., the well and uniform coating of particles in the sample of CZCFA, has been confirmed by the Mössbauer spectra of this sample where a well-defined doublet has been found for the presence of a substantial fraction of lower sizes of SPM particles. The saturation magnetization and saturation-to-remanence ratio of the samples are moderately high, but the coercive field is significantly low. In this direction CZCF sample annealed at 800 °C is quite interesting for its high value of room temperature magnetization, low value of coercive field for its mixed state of SPM and ferrimagnetic particles, square-shaped hysteresis loop, and low hysteresis loss, and these would be suitable for various soft magnetic device applications.

Acknowledgment. The authors thank the DST, Government of India, for the financial support of this work (Project No. SR/S2/CMP-43/2006). S.M. also thanks the DST, Government of India, for providing his fellowship.

References and Notes

(1) Dormann, J. L.; Fiorani, D. *Magnetic Properties of Fine Particles*; North-Holland: Amsterdam, 1992.
(2) Sung, H. M.; Chen, C. J.; Ko, W. S.; Lin, H. C. *IEEE Trans. Magn.* **1994**, *30*, 4906–4908.
(3) Berkowitz, A. E.; Kodama, R. H.; Makhlouf, S. A.; Parker, F. T.; Spada, F. E.; McNiff, E. J., Jr.; Foner, S. *J. Magn. Magn. Mater.* **1999**, *196−197*, 591–594.
(4) *Scientific and Clinical Applications of Magnetic Carriers*; Hafeli, U., Schutt, W., Teller, J., Zborowski, M., Eds.; Plenum Press: New York, 1997.
(5) Kim, W. C.; Kim, S. J.; Lee, S. W.; Kim, C. S. *J. Magn. Magn. Mater.* **2001**, *226−230*, 1418–1420.
(6) Yue, Z.; Zhou, J.; Wang, X.; Gui, Z.; Li, L. *J. Mater. Sci. Lett.* **2001**, *20*, 1327–1329.
(7) Nath, B. K.; Chakrabarti, P. K.; Das, S.; Kumar, U.; Mukhopadhyay, P. K.; Das, D. *Eur. Phys. J. B* **2004**, *39*, 417–425.
(8) Nath, B. K.; Chakrabarti, P. K.; Das, S.; Kumar, U.; Mukhopadhyay, P. K.; Das, D. *J. Surf. Sci.Technol.* **2005**, *21*, 169–182.
(9) Kim, C. S.; Kim, W. C.; An, S. Y.; Lee, S. W. *J. Magn. Magn. Mater.* **2000**, *215−216*, 213–216.
(10) Kryder, M. H. *MRS Bull.* **1996**, *21*, 17–19.
(11) Pardavi-Horvath, M. *J. Magn. Magn. Mater.* **2000**, *215−216*, 171–183.
(12) Moeser, G. D.; Roach, K. A.; Green, W. H.; Laibinis, P. E.; Hatton, T. A. *Ind. Eng. Chem. Res.* **2002**, *41*, 4739–4749.
(13) Sahoo, S. K.; Labhasetwar, V. *Drug Discov. Today* **2003**, *8* (24), 1112–1120.
(14) Gould, P. *Mater. Today* **2004**, *7*, 36–43.
(15) Berkovsky, B. M.; Medvedev, V. F.; Krakov, M. S. *Magnetic Fluids: Engineering Application*; Oxford University Press: Oxford. U.K., 1993.
(16) Berkovsky, B.; Bashtovoi, V. *Magnetic Fluids and Applications Handbook*; Begell House: New York, 1996.
(17) Blums, E.; Cebers, A.; Maiorov, M. M. *Magnetic Fluids*; Walter de Gryuter & Co. (Berlin): New York, 1997.
(18) Rosensweig, R. E. *Ferrohydrodynamics*; Dover Publications: Mineola, NY, 1997.
(19) Chastellain, M.; Petri, A.; Gupta, A.; Rao, K. V.; Hofmann, H. *Adv. Eng. Mater.* **2004**, *6*, 235–241.
(20) Hofer, K. G. *Eur. Cells Mater.* **2002**, *3*, 67–69.
(21) Halbreich, A.; Roger, J.; Pons, J. N.; Geldwerth, D.; Da Silva, M. F.; Roudier, M.; Bacri, J. C. *Biochimie* **1998**, *80*, 379–390.
(22) Ramchand, C. N.; Pande, P.; Kopcansky, P.; Mehta, R. V. *Indian J. Pure Appl. Phys.* **2001**, *39*, 683–686.
(23) Babincova', M.; Leszczynska, D.; Sourivong, P.; Cicmanec, P.; Babinec, P. *J. Magn. Magn. Mater.* **2001**, *225*, 109–112.
(24) Jordan, A.; Scholz, R.; Wust, P.; Schirra, H.; Schiestel, T.; Schmidt, H.; Felix, R. *J. Magn. Magn. Mater.* **1999**, *194*, 185–196.
(25) Mata-Zamoraa, M. E.; Montiela, H.; Alvarezb, G.; Sanigera, J. M.; Zamoranoc, R.; Valenzuelab, R. *J. Magn. Magn. Mater.* **2007**, *316*, e532−e534.
(26) Su, H.; Zhang, H.; Tang, X.; Xiang, X. *J. Magn. Magn. Mater.* **2004**, *283*, 157–163.
(27) Nomura, T.; Takaya, M. *Hybrids* **1987**, *3*, 15.
(28) Yue, Z.; Li, L.; Zhou, J.; Zhang, H.; Ma, Z.; Gui, Z. *Mater. Lett.* **2000**, *44*, 279–283.
(29) Chinnasamy, C. N.; Senoue, M.; Jeyadevan, B.; Perales-perez, O.; Shinoda, K.; Tohji, K. *J. Colloid Interf. Sci.* **2003**, *263*, 80–83.
(30) Lee, J. G.; Park, J. Y.; Kim, C. S. *J. Mater. Sci.* **1998**, *33* (15), 3965–3968.
(31) Victoria, L.; Calero-del, D. C.; Rinaldi, C. *J. Magn. Magn. Mater.* **2007**, *314*, 60–67.
(32) García-Cerda, L. A.; Escarenõ-Castro, M. U.; Salazar-Zertuche, M. *J. Non-Cryst. Solids* **2007**, *353*, 808–810.
(33) Chakrabarti, P. K.; Nath, B. K.; Brahma, S.; Das, S.; Goswami, K.; Kumar, U.; Mukhopadhyay, P. K.; Das, D.; Ammar, M.; Mazaleyrat, F. *J. Phys: Condens. Matter.* **2006**, *18*, 5253–5267.
(34) Chinnasamy, C. N.; Narayanasamy, A.; Ponpandian, N.; Chattopadhyay, K.; Guerault, H.; Gréneche, J.-M. *J. Phys.: Condens. Matter.* **2000**, *12*, 7795–7805.
(35) Pandya, P. B.; Joshi, H. H.; Kulkarni, R. G. *J. Mater. Sci.* **1991**, *26*, 5509–5512.
(36) Modak, S.; Ammar, M.; Mazaleyrat, F.; Das, S.; Chakrabarti, P. K. *J. Alloys Compd.* **2009**, *473*, 15–19.
(37) Chakrabarti, P. K.; Nath, B. K.; Brahma, S.; Das, S.; Ammar, M.; Mazaleyrat, F. *Solid State Commun.* **2007**, *144*, 305–309.
(38) Mukherjee, S.; Acharya, S.; Das, D.; Chakrabarti, P. K. *J. Nanosci. Nanotechnol.* **2010**, *10*, 5623–5633.
(39) Modak, S.; Karan, S.; Roy, S. K.; Mukherjee, S.; Das, D.; Chakrabarti, P. K. *J. Magn. Magn. Mater.* **2009**, *321*, 169–174.

(40) Lebedev, M.; Akedo, J.; Iwata., A.; Sugimoto, S.; Inomata, K. *J. Am. Ceram. Soc.* **2004**, *87*, 1621–1624.

(41) Kim, W. C.; Jin Kim, S.; Uhm, Y. R.; Kim, C. S. *IEEE Trans. Magn.* **2002**, *37*, 2362–2365.

(42) Hu, J.; Yan, M. J. *Zh. Univ. Sci. B.* **2005**, *6*, 580–583.

(43) Ghazanfar, U.; Siddiqi, S. A.; Abbas, G. *Mater. Sci. Eng. B* **2005**, *118*, 84–86.

(44) Mandal, K.; Pan Mandal, S.; Agudo, P.; Pal, M. *Appl. Surf. Sci.* **2001**, *182*, 386–389.

(45) Thakur, S.; Katyal, S. C.; Gupta, A.; Reddy, V. R.; Sharma, S. K.; Knobel, M.; Singh, M. *J. Phys. Chem. C* **2009**, *113*, 20785–20794.

(46) Li, L.; Qiu, H.; Qian, H.; Hao, B.; Liang, X. *J. Phys. Chem. C* **2010**, *114*, 6712–6717.

(47) Hou, C.; Yu, H.; Zhang, Q.; Li, Y.; Wang, H. *J. Alloys Compd.* **2010**, *491*, 431–435.

(48) Brand, R. A. *Nucl. Instrum. Methods Phys. Res., Sect. B* **1987**, *28*, 398–416.

JP104535V